Toward a quantitative evaluation of the strength of Cp2M×××η 2–borate interactions

Jingwen Zhu, Emilie-Laure Zins, Mohammad Esmaïl Alikhani

Toward a quantitative evaluation of the strength of $Cp_2M\cdots\eta^2$-borate interactions

Jingwen Zhu, Emilie-Laure Zins, Mohammad Esmaïl Alikhani

Sorbonne Universités, UPMC Univ. Paris 06, CNRS, De la Molécule aux Nano-objets : Réactivité, Interactions et Spectroscopies (MONARIS), Equipe de Modélisation et Chimie Théorique (E=MCT), UMR 8233, Université Pierre et Marie Curie, 4 Place Jussieu, case courrier 49, F-75252 Paris Cedex 05, France

Abstract

Amine boranes might be a crucial material toward a successful energy transition. A precise description of metal-ligand interactions involved in the homogeneous catalysis of the dehydrogenation of amine boranes would represent a major step toward a global understanding of the reaction process. η^2 interactions between borates and organometallic compounds were identified as key intermediates in the reaction pathways. Herein are proposed reduced topological descriptors to measure the efficiency of several metallocenes to activate B-H bonds in prototypical $Cp_2M\cdots\eta^2$-borates complexes. The combined use of QTAIM and ELF partitions allowed us to ascertain the 3C/2e interactions between borates and metallocenes. The strength of the B-H bond is affected by two different parameters: the nature of the ligands bonded to the borates and the effect of the interaction with the metallocene. The use of reduced descriptors allows to evaluate the activation of the B-H bond due to the sole effect of the interaction between the borates and the metallocenes. Herein, we suggest the concomitant use of the reduced electron density $\frac{\rho(BCP\ B-H_{complex})}{\rho(BCP\ B-H_{free\ borate})}$ and reduced distance $\frac{d(B-H_{complex})}{d(BCP\ B-H_{free\ borate})}$ of the B-H bonds to classify the {borates + metallocenes} systems as a function of the strength of the B-H interaction with the metallocene. We further suggest to complement this evaluation based on the QTAIM analysis by a quantization of the contribution of the metallic center on the protonated basin defined within the ELF framework.

Introduction

Energy transition is one of the main challenges facing catalytic chemistry. Studies are still in progress to propose hydrogen-economy sustainable solutions.[1] Amine boranes and related compounds constitute attractive targets as clean hydrogen sources via catalytic dehydrogenation/dehydrocoupling reactions. Numerous studies have demonstrated their potentials as hydrogen sources.[2-8] A precise understanding of the reaction mechanisms would help in designing new catalytic approaches.[9-11] Furthermore, a screening of a large panel of {catalyst + substituted amine boranes} systems would help in finding a highly efficient dehydrogenation process. *In silico* studies are particularly attractive for such screening. Moreover, recent advances in DFT methods in combination with the increase of computational resources make it possible to study whole reaction mechanisms of catalytic dehydrocoupling.[12-14] However, some of the results thus obtained are hardly comparable with experiments, because of the intricacies of the real reaction pathways, that may involve several catalytic cycles, unidentified catalytic species, multi-coordination of reagents, solvated species, and other aspects that are hardly considered in computational investigations.[15] Complementarily to complete studies of the reaction pathways, specific descriptors may be used to characterize bond activations in reaction intermediates. Such approach was previously applied to the characterization of C-H bond activations in the context of agostic interactions.[16] As far as the dehydrogenation/dehydrocoupling of amine boranes is concerned, there is a consensus that 3 center/2 electron (3C/2e) interactions play a prominent role in the dehydrogenation process of amine borane compounds.[2] This includes the formation of B-H (intramolecular) agostic interactions, as well as intermolecular η^2-hydroborate interactions, and the formation of Kubas complexes. [2,17-23]

The aim of the present study is to propose specific descriptors that would allow a comparison of the strength of intermolecular interactions between borate anions and metallocene cations. Borates interacting with metallocenes were chosen as simple prototypes, to identify specific topological descriptors based on the quantum theory of atoms in molecules (QTAIM)[24,25] and the electron localization function (ELF) [26] topological analyses.

Why using topological descriptors?

As a first approximation, the experimentally determined B-H and M-H distances could be considered as simple indicators of the strength of the interaction. A lengthening of the B-H bond, combined with a relatively short distance M-H should be an indicator of a strong interaction. But the graph plotted in **Figure 1** clearly demonstrates that these simple indicators do not allow an easy classification of the {borates + metallocenes} systems according to the force of interaction. This can be explained by several aspects: i) a physico-chemical phenomenon: the nature of the metallic center and the ligand influence the interaction and the different {borates + metallocenes} systems cannot be directly compared; ii) a technical phenomenon: the experimental determination of the M-H and B-H distances by X-ray diffraction is entangled by an error due to the difficulty in locating H atoms; and iii) The size of sample is really limited and the properties of these selected systems are similar.

Table 1: Characteristic distances between interacting atoms in the $Cp_2M^{\cdots}\eta^2$-borate complexes. Experimental (DRX, values taken from the literature) and calculated (B3LYP/6-311++G(2d,2p)+LanL2DZ level of theory, present study) distances.

Complex		M-H···B (Å)	B-H···M (Å)
$Cp_2Ti\_H_2BH_2$	Exp[27]	1.75(8)/1.75(8)	1.23(8)/1.23(8)
	Cal	1.897/1.897	1.270/1.270
$Cp_2Ti\_H_2BC_4H_8$	Exp[28]	1.83(3)/1.84(3)	1.23(3)/1.27(3)
	Cal	1.875/1.875	1.290/1.290
$Cp_2Ti\_H_2BC_5H_{10}$	Exp[28]	1.88(3)/1.88(4)	1.18(3)/1.35(3)
	Cal	1.891/1.889	1.300/1.295
$Cp_2Ti\_H_2BC_8H_{14}$	Exp[28]	1.89(2)/1.90(1)	1.23(1)/1.29(2)
	Cal	1.892/1.892	1.292/1.292
$Cp_2Ti\_H_2B(C_6F_5)_2$	Exp[29]	1.973/2.031	1.320/1.320
	Cal	1.963/1.963	1.254/1.254

Complex		M-H···B (Å)	B-H···M (Å)
$Cp_2Nb\_H_2BH_2$	Exp[28]	1.83(4)/1.83(4)	1.39(4)/1.39(4)
	Cal	1.921/1.921	1.313/1.312
$Cp_2Nb\_H_2BC_4H_8$	Exp[28]	1.82(3)/1.76(3)	1.30(3)/1.27(3)
	Cal	1.899/1.899	1.339/1.339
$Cp_2Nb\_H_2BC_5H_{10}$	Exp[28]	1.85(3)/1.85(3)	1.26(3)/1.26(3)
	Cal	1.915/1.911	1.345/1.341
$Cp_2Nb\_H_2BC_8H_{14}$	Exp[28]	1.87(4)/1.89(4)	1.32(3)/1.26(3)
	Cal	1.916/1.916	1.335/1.335

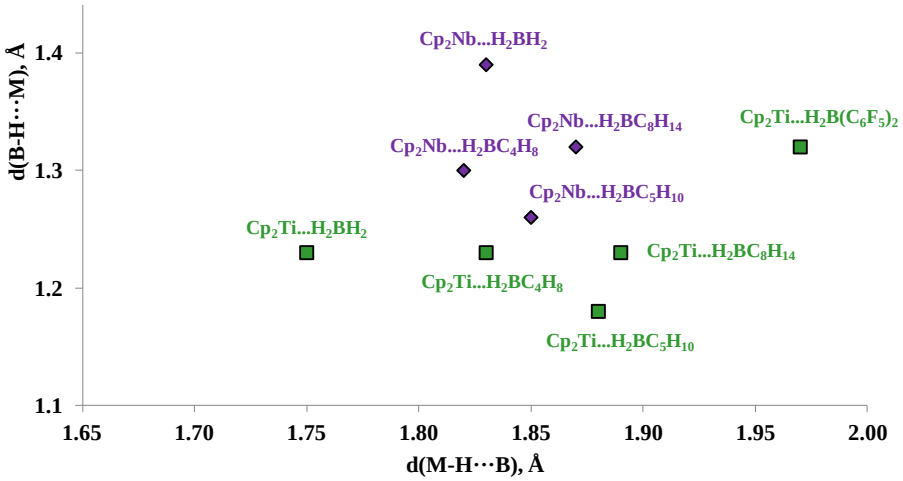

Figure 1: Comparison of the experimental B-H and M-H distances in the complexes studied by means of X-ray diffraction (values taken from the literature).

Since simple geometric considerations are not sufficient to shed some light on role of the metallocene on the B-H bond activation, the use of topological tools is worth considering. Previous studies have demonstrated the usefulness of topological descriptors based on the QTAIM[30,31] and ELF[32] topological analyses to analyze bond activations in organometallic complexes. Such approach was previously applied to the study of C-H bond activation in so-called agostic interactions. Based on the electron density $\rho(r)$, the QTAIM analysis allows the localization of the atoms in the molecule, as well as a characterization of chemical bonds. The identification of a bond path (BP) together with a bond critical point (BCP) between two atoms is the (qualitative) signature of a bonding. Furthermore, the properties of the electron density function at the BCP (the values of $\rho(r)$, its Laplacian $\nabla^2\rho(r)$, the ellipticity ε and the total energy density H) allows a quantitative characterization of the bonding. It was demonstrated that the QTAIM framework leads to an efficient identification of β agostic bondings. [33] However, α agostic bondings cannot be characterized by such approaches [34] (with the exception of bridged α agostic bondings[35]).

The ELF topological analysis relies in the use of a function of the electron density.[36] Its use leads to the identification of core and valence basins. When combined with the QTAIM definition of atoms, the contribution of each atom in a definite basin can be quantified. The ELF signature on a C-H agostic interaction should consist in a protonated basin containing ≈ 2e belonging to three atoms: the metallic center, the carbon atom and the hydrogen atom.[16]

Finally, several descriptors were selected as specific markers of the strength of the C-H agostic interaction. It was also shown that such an approach can also be applied to the study of the strength of σ B-H agostic interactions.[16] The present study aims at developing relevant topological descriptors that may help in choosing ligands and metallocenes leading to an enhanced B-H bond activation.

In order to further shed some light on possible effects due to the nature of the substituents bonded to the borates and the nature of the metal atom, additional compounds were also considered. Finally, a set of 29 $Cp_2M\cdots\eta^2$-borate complexes (M = Ti, Zr, V, Nb) was investigated for the present study (**Figure 2**). Titanocenes and zirconocenes with a spin multiplicity of 2 and niobiocenes and vanadocenes with a spin multiplicity of 1 were considered in the present study.

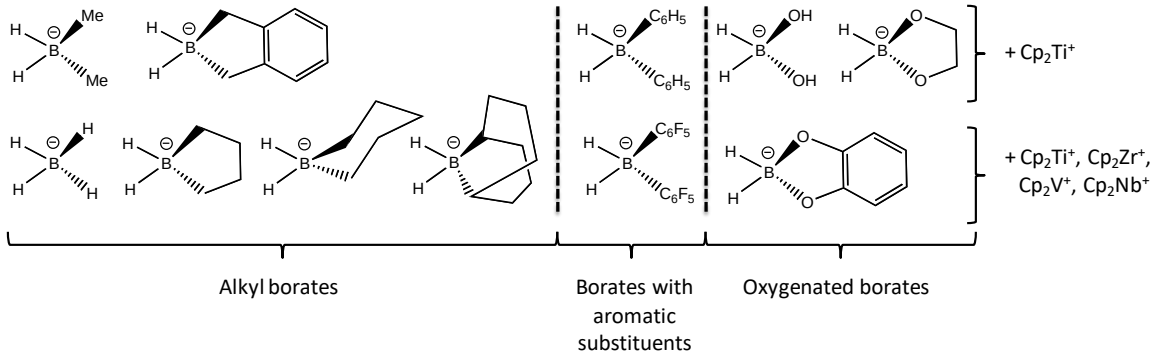

Figure 2: Ligands and metallocenes that were selected for the present study of $Cp_2M\cdots\eta^2$-borate interactions.

Computational details

All the geometry optimizations were carried out using the Gaussian09 software.[37]

A previous study has shown that B-H intramolecular agostic interactions with metallocenes are satisfactorily depicted using the following approach:[38]

- geometry optimization using the three-parameter hybrid B3LYP[39,40] functional, in combination with the 6-311++G(2d,2p) basis set for main-group atoms (H, C and B), and the LanL2DZ pseudopotential for the metal centers (Ti, Z, V and Nb). This level of theory will be further referenced as B3LYP/6-311++G(2d,2p)+LanL2DZ,
- geometry optimization is followed by a single-point calculation using the DKH2 (second order Douglas-Kroll-Hess) relativistic Hamiltonian. The DKH2 relativistic Hamiltonian is used in combination with the B3LYP functional (B3LYP-DKH2), and with the all-electron contracted basis set for Douglas-Kroll-Hess calculation: DZP-DKH[41-43] basis set for all atoms to take into account core electrons in the topological analysis. The .wfn files required for the topological analysis are generated during this step.

The same level of theory was chosen for the present study. Complementarily, the effect of the D3 empirical correction of Grimme with Becke and Johnson damping [44] on the description of the $Cp_2Ti\cdots\eta^2$-borate interactions was evaluated. As shown in Supporting Information 1, the use of the GD3-BJ empirical correction does not affect the description of the interaction. This may be due to three different reasons:

- the interaction may be correctly calculated with the chosen level of theory,
- the GD3-BJ empirical correction was not particularly fitted on complexes with metal centers,
- the GD3-BJ empirical correction does not correct the electron density.

All the geometry optimizations were carried out with the Gaussian 09 Rev D.01 software. The .wfn files were generated from single point calculations. The Multiwfn software[45] was further used for the topological analysis. The ELF analyses were carried out using the "fine" grid. As far as the QTAIM calculations are concerned, we should point out the fact that the energy densities are evaluated from the Kohn-Sham first reduced density matrix. The values of the electron densities are given in e a.u.$^{-3}$ throughout the text.

For our prospective study, selected geometric parameters that were previously determined by means of X-ray diffraction analysis are reported in Table 1, together with the geometric parameters calculated at the B3LYP/6-311++G(2d,2p)+LanL2DZ level of theory. The close agreement with the experimental and calculated geometries suggests that the chosen level of theory satisfactorily reproduces the geometric features of $Cp_2M \cdots \eta^2$-borate complexes.

Results and discussion

The topological analysis demonstrates the formation of two 3C/2e interactions between borates and metallocenes, for all the {borates + metallocenes} systems studied. The contribution of the valence electrons of the metal atom within the protonated basin is within the [0.05 e; 0.16 e] range, and the total population of the protonated basin is within the [1.90 e; 2.08 e] range. (Supporting Information 2) Furthermore, the QTAIM analysis leads to the identification of a BCP and a bond path between the metal center and the hydrogen atoms for each of these interactions, as shown in **Figure 3**.

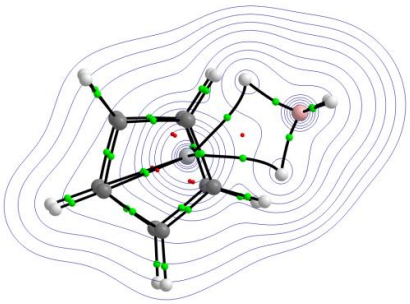

Figure 3: Identification of bond paths and bond critical points between hydrogen atoms of the borate ion and the metal center in the [$Cp_2Ti(\eta^2H_2BH_2)$] complex.

Three topological quantities are worth studying to quantitatively characterize interactions between borates and metallocenes:

i. ρ^{BCP}(B-H): The comparison of ρ^{BCP}(B-H) makes it possible to identify the most reactive B-H bonds, which will be easily broken,

ii. ρ^{BCP}(M-H) which makes it possible to characterize the force of the interaction between the metal center and the σ B-H bond,

iii. The contribution of the metal center (C(M)) to the population of the protonated basin (V(H)), for a global analysis of the interaction.

In the following sub-sections, each of these topological quantities will be used to track the influence of substituents on the borate as well as the influence of the nature of the metallocene on the interaction.

i. a Electronic density at the bond critical point of the σ B-H bonding in $Cp_2Ti \cdots \eta^2$-borate complexes

The weakening of B-H bonds is a determining factor in a borate dehydrogenation process. To investigate the influence of borate substituents on this weakening, we studied the 11 borates interacting with titanocene. **Figure 4** shows the variations of ρ^{BCP}(B-H) as a function of the length of the B-H bond. This direct comparison of the ligands is of interest to the experimenter, since it directly reflects the propensity of the B-H bond to be broken. The longer the B-H bond, the lower the electronic density at the BCP of the bond, the more reactive the B-H bond will be. This graphical representation makes it possible to classify the borates depending on the activation of the B-H bond. Three families of ligands are identified: $H_2BC_xR_y^-$ ligands (with R = H, F) on the one hand, $H_2B(OC_xH_y)_2^-$ ligands on the other hand, and the $H_2BH_2^-$ ligand.

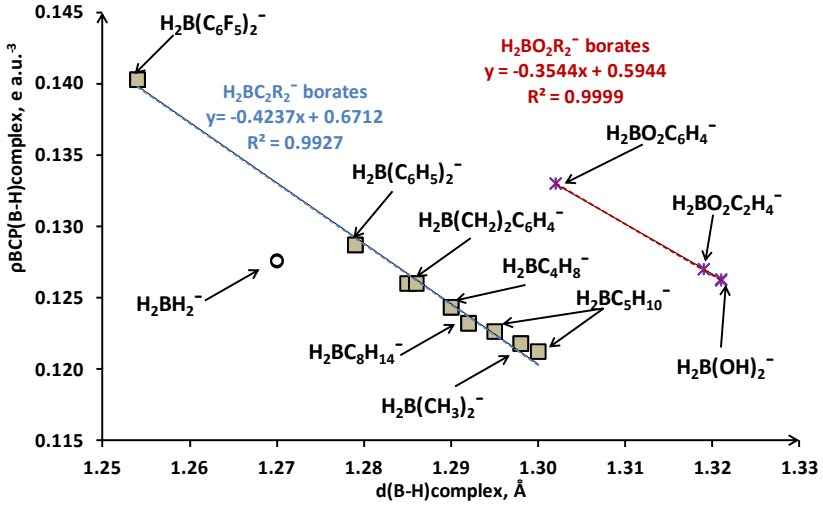

Figure 4: Effect of substituents bonded to the borate on the strength of the B-H bond.

Let us first consider the $H_2BC_xR_y^-$ ligands. When complexed with the titanocene, the B-H bond is the strongest (and thus less reactive) for the two ligands containing aromatic substituents, and the activation of the B-H bond is particularly weak in the $H_2B(C_6F_5)_2^-$ borate. Borates $H_2BC_4H_8^-$, $H_2BC_5H_{10}^-$, $H_2BC_8H_{14}^-$ and $H_2B(CH_3)_2^-$ are those for which the B-H bond is the weakest, which means more likely to react.

Three $H_2B(OC_xH_y)_2^-$ ligands containing B-O bonds were considered in our study: one with an aromatic ring between the two oxygen atoms, one with an aliphatic ring between the two oxygen atoms, and the dihydroxyborate. The dihydroxyborate interacting with the titanocene is the compound having the weakest B-H bond. Conversely, the B-H bond will be less likely to break in the complex formed with $H_2BO_2C_6H_4^-$ compound compared to other $H_2B(OC_xH_y)_2^-$ ligands herein considered.

The strength of the B-H bond in the complexes involves two effects: the intrinsic effect of borate (ie the influence of the nature of the substituent on the B-H bond in the isolated borate) and the effect of the intermolecular interaction with titanocene. In simple Chemist's concepts, these effects correspond to the electronic effects of the substituent groups and electrostatic interaction between cationic metallocene and anionic $H_2BR_2^-$ ligands, respectively.

Figure 5 allows the comparison of the strength of B-H bonds in isolated borates.

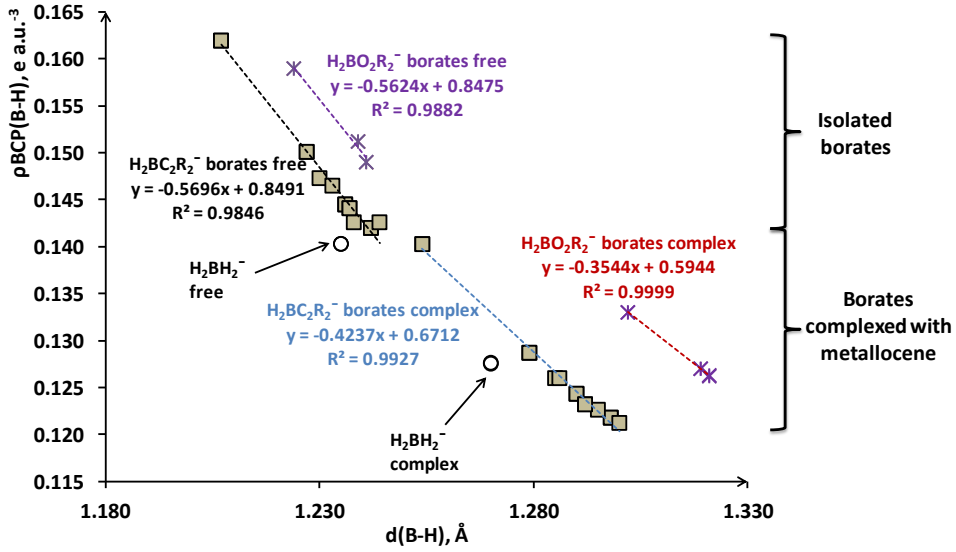

Figure 5: Effects of the substituent on the strength of B-H bonds for isolated borates and for borates interacting with the titanocene cation.

The presence of a relatively strong electrostatic interaction between cationic titanocene and anionic borate in cooperation with a metal-ligand interaction leads to an activation of the B-H covalent bond. When the variation of ρ^{BCP}(B-H) is plotted as a function of the length of the B-H bond, three families of borates can be identified for isolated borates anions (Figure 6): the $H_2BC_2R_2^-$ compounds, the $H_2BO_2R_2^-$ compounds, and the tetrahydroborate anion.

When interacting with the titanocene cation, a right and down shift of these three families is observed (**Figure 5**). Thus, the interaction of the borates anions with the titanocene cation leads to a lengthening of the B-H bond with a concomitant decrease of ρ^{BCP}(B-H).

To further characterize the effect of the intermolecular interaction with titanocene on the activation of the B-H bond, the use of reduced descriptors is particularly relevant. The relevance of such reduced descriptors has already been demonstrated in a comparative study of the strength of agostic intramolecular C-H (and B-H) interactions. In the present study, we sought to extend this approach to the characterization of 3C/2e interactions between borates and titanocene. The weakening of the B-H bonds due to the interaction between the titanocene and borates can be quantified by comparing ρ^{BCP}(B-H) and d(B-H) in the complex and in the free borate. This comparison led us to introduce the following two reduced quantities:

$$\frac{\rho(BCP\ B{-}H_{complex})}{\rho(BCP\ B{-}H_{free\ borate})} \quad \text{and} \quad \frac{d(B{-}H_{complex})}{d(BCP\ B{-}H_{free\ borate})}$$

For all the $H_2BC_xR_y^-$ and $H_2B(OC_xH_y)_2^-$ ligands, the $\frac{\rho(BCP\ B{-}H_{complex})}{\rho(BCP\ B{-}H_{free\ borate})}$ ratio varies linearly with the $\frac{d(B{-}H_{complex})}{d(BCP\ B{-}H_{free\ borate})}$ ratio (**Figure 6**).

In the case of tetrahydroborate, the B-H bond is little affected by the interaction with the titanocene. In all other cases, the interaction between titanocene and borate leads to an increase in the reactivity of the B-H bond, relative to the free borate. The use of reduced quantities makes it possible to demonstrate a higher activation of the B-H bonds in oxygenated borates ($H_2BO_2C_6H_4^-$, $H_2BO_2C_2H_4^-$, and $H_2B(OH)_2^-$) with respect to alkyl borates ($H_2B(CH_2)_2C_6H_4^-$, $H_2BC_4H_8^-$, and $H_2B(CH_3)_2^-$, respectively). The activation of the B-H bond is weaker in the case of borates bearing aromatic substituents (particularly in the case of the $H_2B(C_6F_5)_2^-$ borate).

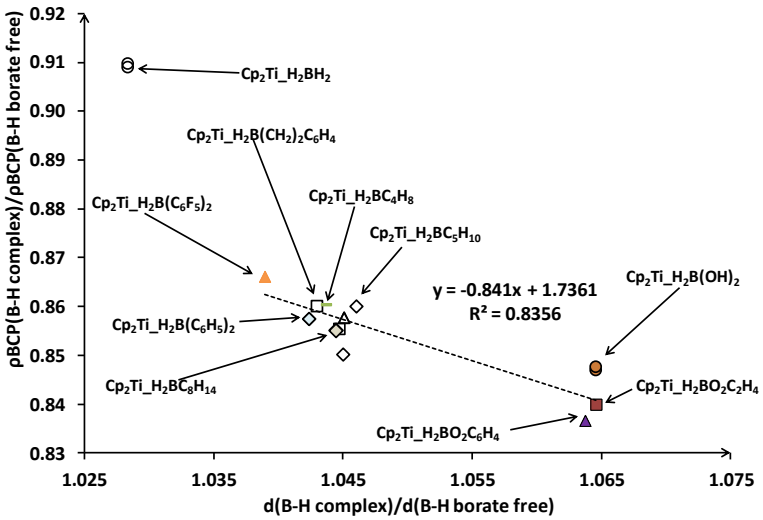

Figure 6: Influence of the $Cp_2Ti^{\cdots}\eta^2$-borate interaction on the strength of the B-H bond.

i. b Influence of the metallic center on the electronic density at the bond critical point of the σ B-H bonding in $Cp_2M^{\cdots}\eta^2$-borate complexes

Besides the effect of substituents on the borate, the question of the impact of the metallocene on the B-H bond activation should also be addressed. The variations of $\frac{\rho(BCP\ B{-}H_{complex})}{\rho(BCP\ B{-}H_{free\ borate})}$ were plotted as a function of $\frac{d(B{-}H_{complex})}{d(BCP\ B{-}H_{free\ borate})}$ for all the 29 {borates + metallocenes} systems considered in the present study (**Figure 7**).

When the 29 complexes are considered altogether, the use of the reduced quantities leads to the identification of two populations of complexes: the tetrahydroborates interacting with the metallocenes on the one hand, and the di-substituted borates interacting with the metallocenes on the other hand. The B-H bonds of the tetrahydroborate are systematically less influenced by the interaction with the metallocene compared with the di-substituted borates, whatever the nature of the metallocene is: the electron density at BCP and the length of the bond in the complexes are

close to those of the free borate. In the case of di-substituted borates, the interaction with the metallocenes results in a weakening of the B-H bonds: the bonds are elongated and the electron density at BCP decreases. Furthermore, for a given borate, activation of the B-H bond increases from titanocene to zirconocene to vanadocene and niobiocene. Thus the use of the niobiocene could be an interesting alternative to catalyze the dehydrogenation process of borates.

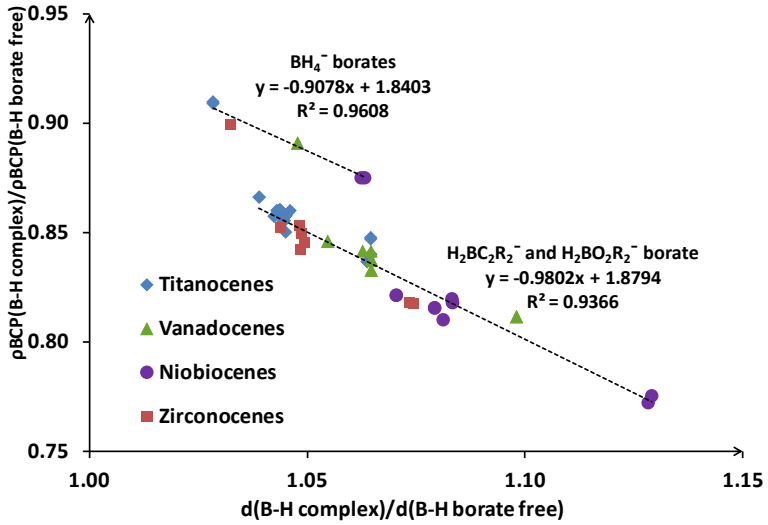

Figure 7: Influence of the Cp2M··· η²-borate interaction on the strength of the B-H bond.

ii. a Electronic density at the bond critical point of the M-H bonding in Cp_2Ti ··· η²-borate complexes

In all the cases studied, the QTAIM analysis of the interactions between borates and metallocenes leads to the identification of bond paths as well as BCPs between hydrogen atoms and the metal center. The strength of the interaction can therefore be evaluated by following the evolution of ρ^{BCP}(M-H) as a function of the M-H distance. **Figure 8** presents the results obtained for the borates interacting with titanocene: ρ^{BCP}(M-H) decreases linearly with the distance M-H, whatever the nature of the substituents on the borate is. The interaction is strongest with the oxygenated borates ($H_2B(OH)_2^-$, $H_2BO_2C_2H_4^-$ and $H_2BO_2C_6H_4^-$) with respect to alkyl borates, and a weaker interaction is identified with borates bearing aromatic substituents, with a particularly weak interaction in the case of the $H_2B(C_6F_5)_2^-$ borates.

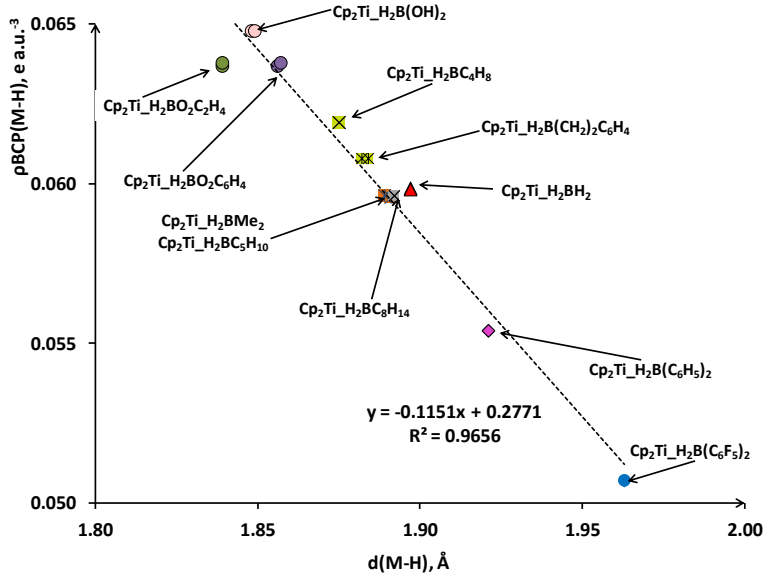

Figure 8 : Quantization of the strength of the M-H interaction for differently substituted borates interacting with the titanocene.

A general trend is evident regarding the effect of nature of substituents bonded to the borate. Furthermore, the stronger the B-H interaction with the metal center is, the more weakened the B-H bond is (Scheme 1).

Scheme 1: Influence of the nature of substituents bonded to the boron atom on the strength of the interaction.

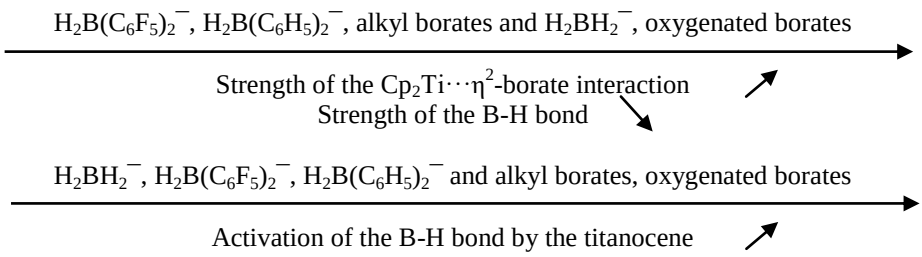

ii. b Influence of the metallic center on the electronic density at the bond critical point of the M-H bonding in $Cp_2M\cdots\eta^2$-borate complexes

When the nature of the metal center is modified, the strongest M-H interactions are systematically observed with the oxygenated substituents, and the weakest interactions with the aromatic substituents (**Figure 9**). For a given borate, the QTAIM analysis of the BCP(M-H) suggests that the $Cp_2M\cdots\eta^2$-borate interactions are systematically stronger with vanadocenes (respectively niobiocenes) compared to titanocenes (respectively zirconocenes).

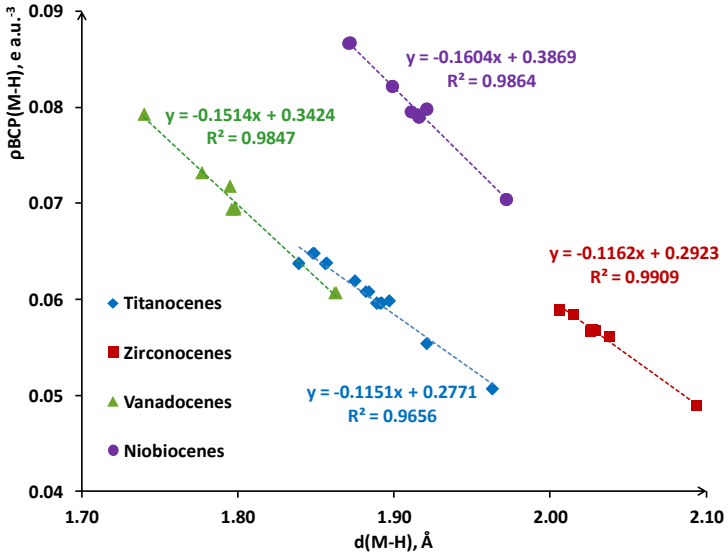

Figure 9: Influence of the metal center on the strength of the M-H interaction.

iii. a Global analysis of the $Cp_2M\cdots\eta^2$-borate interaction

The topological characterizations of the B-H bond and M···H interactions are complementary in these $Cp_2Ti\cdots\eta^2$-borate complexes: the geometrical (distance) and electronic (ρ^{BCP}) characteristics of the B-H bonds will play a fundamental role in the reactivity, whereas the M-H distance and ρ^{BCP}(M-H) are direct measurements of the strength of the interaction with the metal center. However, the QTAIM analysis of the B-H and M-H bond paths is not sufficient for a full quantitative description of these 3C/2e interactions. The ELF analysis allow to quantify the contribution of the metallic center (C(M)) within the protonated basin (V(H)) involved in the 3C/2e interactions. The use of the following reduced topological and geometric quantities have already been introduced to classify σ C-H agostic interactions involved in different {borates + metallocenes} systems[16]:

$$100 \times \frac{C(M)}{V(H)} \text{ and } \frac{d(C-H)}{d(M-H)}$$

In the present study, these reduced descriptors were used to further characterize the $Cp_2M\cdots\eta^2$-borate interaction. The graphical representation $100 \times \frac{C(M)}{V(H)} = f\left[\frac{d(B-H)}{d(M-H)}\right]$ allows classifying the borates in their order of increasing interaction with the titanocene (**Figure 10**):

- The $H_2B(C_6F_5)_2^-$ borate is the one for which the interaction with the titanocene is the weakest,
- Thereafter $H_2B(C_6H_5)_2^-$ and BH_4^- borates are characterized by a similar normalized contribution of the metallic center within the protonated basins,
- All alkyl borates comparably interact with the titanocene,

- The oxygenated borates systematically lead to the strongest interactions with titanocene.

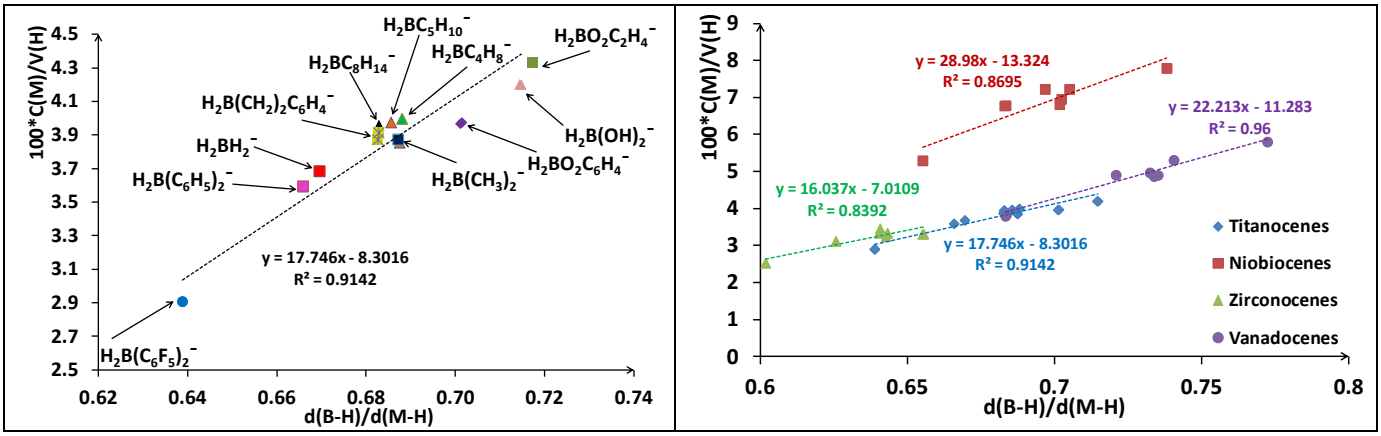

Figure 10 : Global evaluation of the $Cp_2M^{\cdots}\eta^2$-borate interaction.

The classification thus obtained is similar to that deduced from the graphical representation of the variations of ρ^{BCP}(M-H) as a function of (M-H). Thus the use of oxygenated borates should favor the dehydrogenation step with titanocenes, whereas aromatic borates inhibit the reaction. Similar results are obtained with zirconocene, vanadocene and niobiocene: the presence of B-O bonds in the borates results in stronger $Cp_2M\cdots\eta^2$-borate interactions that should favor the dehydrogenation processes.

It is interesting to compare the scale of $Cp_2M\cdots\eta^2$-borate interactions thus obtained with an orbital approach. To predict the propensity of different borates to interact with a given metallocene cation using this approach, the energies of the highest occupied molecular orbitals (HOMOs) should be considered. The highest the HOMO of an isolated borate is, the easier the interaction with the metallocene will be. The energies of the HOMOs of all the isolated borates anions considered in the present study are reported in Table 2. The $H_2B(C_6F_5)_2^-$ borate is found to have a lowest HOMO value at -0.138 a.u. while the HOMOs of the oxygenated borates lies higher, at -0.028 a.u.. The aliphatic borates have a HOMO value in the [-0.071 a.u.; -0.059 a.u.] range (Table 2).
Thus, using such an approach, the oxygenated borates are predicted to form stronger interactions with a given metallocene. Conversely, the aromatic borates are predicted to form weaker interactions with a given metallocene. This classification is consistent with the one obtained using the topological descriptors.

Table 2 : Energies of the HOMO (Highest Occupied Molecular Orbital) of each isolated borate anion.

Ligands	Energy of HOMO (a.u.)
$H_2BO_2C_2H_4^-$	-0.028
$H_2BO_2C_6H_4^-$	-0.029
$H_2B(OH)_2^-$	-0.039
$H_2BMe_2^-$	-0.059
$H_2BC_4H_8^-$	-0.063
$H_2BC_8H_{14}^-$	-0.063
$H_2BC_5H_{10}^-$	-0.066
BH_4^-	-0.066
$H_2B(CH_2)_2C_6H_4^-$	-0.071
$H_2B(C_6H_5)_2^-$	-0.091
$H_2B(C_6F_5)_2^-$	-0.138

Conclusion

We have proposed an approach to qualitatively and quantitatively describe the η^2 interaction between borates anions and organometallic complexes. From a qualitative point of view, the ELF analysis is useful to ascertain the presence

of two electrons in the protonated basins involved in the interaction. The origin of these two electrons is further analyzed thanks to the QTAIM definition of atoms in molecules. In all the {borates + metallocenes} systems herein studied, the η^2 interactions were found to be 3C/2e interactions, with a non-negligible participation of the valence electrons of the metal atom within the protonated basins ($C(M) \geq 0.05$ e). The quantitative analysis of the strength of the interactions is simplified by the presence of bond paths and BCPs between the metal atom and both hydrogen atoms of the η^2-borates within the QTAIM framework. The concomitant use of the ρ^{BCP}(B-H) and d(B-H) descriptors is particularly useful to classify the {borates + metallocenes} systems depending on the propensity of borate to undergo dehydrogenation processes. The study of free borates leads to the definition of two reduced descriptors: the reduced electron density $\frac{\rho(BCP\ B-H_{complex})}{\rho(BCP\ B-H_{free\ borate})}$ and reduced distance $\frac{d(B-H_{complex})}{d(BCP\ B-H_{free\ borate})}$. The concomitant use of these two reduced descriptors leads to a QTAIM classification of the {borates + metallocenes} systems as a function of the strength of the B-H interaction with the metallocene: when the boron atom is bonded to oxygen atoms, the $Cp_2M\cdots\eta^2$-borate interaction lead to the most activated B-H bonds. Conversely, the B-H bonds of the $Cp_2M\cdots\eta^2$-$H_2B(C_6F_5)_2$ complexes are the less activated ones. Furthermore, the higher the contribution of the valence electrons of the metal center within the protonated basins is, the stronger the 3C/2e interaction is. Thus, the study of the $100 \times \frac{C(M)}{V(H)}$ reduced ELF descriptor as a function of the $\frac{d(B-H)}{d(M-H)}$ reduced distance is another way to characterize the $Cp_2M\cdots\eta^2$-borate interaction. The ELF classification of the {borates + metallocenes} systems as a function of the strength of the interaction is similar to the QTAIM classification: the presence of B-O bonds enhances the activation of B-H bonds due to the $Cp_2M\cdots\eta^2$-borate interactions. The interaction scale thus obtained is also in line with electronic effects that may be described in terms of inductive and mesomeric effects familiar to chemists. This methodological work on prototype systems has set the basis for further investigations of the B-H bond activation of amine boranes by organometallic complexes.

(1)Zhang, F., Zhao, P., Niu, M., & Maddy, J. The survey of key technologies in hydrogen energy storage. *International Journal of Hydrogen Energy*. **2016**, 41, 14535-14552.

(2) Johnson, H. C.; Hooper, T. N.; Weller, A. S. The catalytic dehydrocoupling of amine–boranes and phosphine–boranes. In Synthesis and Application of Organoboron Compounds. *Springer International Publishing*. **2015,** 153-220.

(3) Demirci, U. B. Ammonia borane, a material with exceptional properties for chemical hydrogen storage. *International Journal of Hydrogen Energy*. **2017**, 42, 9978-10013.

(4) Rossin, A., & Peruzzini, M. Ammonia–Borane and Amine–Borane Dehydrogenation Mediated by Complex Metal Hydrides. *Chem. Rev*, **2016**, 116, 8848-8872.

(5) Bhunya, S., Malakar, T., Ganguly, G., & Paul, A. Combining Protons and Hydrides by Homogeneous Catalysis for Controlling the Release of Hydrogen from Ammonia–Borane: Present Status and Challenges. *ACS Catalysis*, **2016**, 6, 7907-7934.

(6) Zhan, W. W., Zhu, Q. L., & Xu, Q. Dehydrogenation of ammonia borane by metal nanoparticle catalysts. *ACS Catalysis*, **2016**, 6, 6892-6905.

(7) Ren, J., Musyoka, N. M., Langmi, H. W., Mathe, M., & Liao, S. Current research trends and perspectives on materials-based hydrogen storage solutions: a critical review. *International Journal of Hydrogen Energy*. **2017**, 42, 289-311

(8) Mahato, S., Banerjee, B., Pugazhenthi, G., & Banerjee, T. Optimization and quantum chemical predictions for the dehydrogenation kinetics of Ammonia Borane–Ionic Liquid mixtures. *International Journal of Hydrogen Energy*, **2015**, 40, 10390-10400.

(9) Cheng, G. J., Zhang, X., Chung, L. W., Xu, L., & Wu, Y. D. Computational organic chemistry: bridging theory and experiment in establishing the mechanisms of chemical reactions. *Journal of the American Chemical Society*, **2015**, 137, 1706-1725.

(10) Spivey, J. J., Krishna, K. S., Kumar, C. S., Dooley, K. M., Flake, J. C., Haber, L. H. et al.. Synthesis, characterization, and computation of catalysts at the center for atomic-level catalyst design. *The Journal of Physical Chemistry C*, **2014**, 118, 20043-20069.

(11) Klippenstein, S. J., Pande, V. S., & Truhlar, D. G. Chemical kinetics and mechanisms of complex systems: a perspective on recent theoretical advances. *Journal of the American Chemical Society*, **2014**, 136, 528-546.

(12) Bhunya, S., & Paul, A. Designing an effective Metal free Lewis acid catalyst for Ammonia-borane Dehydrogenation: A DFT Investigation on Triarylboranes. *ChemCatChem*. . **2017**, DOI: 10.1002/cctc.201700416

(13) Zhou, T., Wang, G., Cui, H., Yuan, H., Kuang, A., Tian, C. et al.. A novel dehydrogenation style of NH_3BH_3 by catalyst of transition metal clusters. *International Journal of Hydrogen Energy*, **2016**, 41, 11746-11760.

(14) Sicilia, E. Computation modeling as a tool for the exploration of complex multistep reaction cycles in homogeneous catalysis. Some selected examples in the framework of the use of hydrogen as a fuel of the future. *International Journal of Quantum Chemistry*, **2016**, 116, 1507-1512.
(15) Pidko, E.A. Towards the balance between the reductionist and systems approaches in computational catalysis: model versus method accuracy for the description of catalytic systems. *ACS Catalysis*. **2017**, 7, 4230–4234
(16) Zins, E. L.; Silvi, B.; Alikhani, M. E. Activation of C–H and B–H bonds through agostic bonding: an ELF/QTAIM insight. *Phys. Chem. Chem. Phys.* **2015,** 17, 9258-9281.
(17) Alcaraz, G.; Sabo-Etienne, S. Coordination and dehydrogenation of amine–boranes at metal centers. *Angew. Chem. Int. Ed.* **2010,** 49, 7170-7179.
(18) Stevens, C. J.; Dallanegra, R.; Chaplin, A. B.; Weller, A. S.; Macgregor, S. A.; Ward, B.; Sabo-Etienne, S. $[Ir(PCy_3)_2(H)_2(H_2BNMe_2)]^+$ as a Latent Source of Aminoborane: Probing the Role of Metal in the Dehydrocoupling of H_3BNMe_2H and Retrodimerisation of $[H_2BNMe_2]_2$. *Chem. Eur. J.* **2011,** 17, 3011-3020.
(19) Dallanegra, R.; Chaplin, A. B.; Tsim, J.; Weller, A. S. Amino-borane oligomers bound to a Rh (I) metal fragment. *Chem. Commun.* **2010,** 46, 3092-3094.
(20) Tang, C. Y.; Thompson, A. L.; Aldridge, S. Dehydrogenation of saturated CC and BN bonds at cationic N-heterocyclic carbene stabilized M (III) centers (M= Rh, Ir). *J. Am. Chem.Soc.* **2010,** 132, 10578-10591.
(21) Dallanegra, R.; Robertson, A. P.; Chaplin, A. B.; Manners, I.; Weller, A. S. Tuning the $[L_2Rh\cdots H_3B\cdot NR_3]$+ interaction using phosphine bite angle. Demonstration by the catalytic formation of polyaminoboranes. *Chem. Commun.* **2011,** 47, 3763-3765.
(22) Douglas, T. M.; Chaplin, A. B.; Weller, A. S.; Yang, X.; Hall, M. B. Monomeric and oligomeric amine− borane σ-complexes of rhodium. Intermediates in the catalytic dehydrogenation of amine− boranes. *J. Am. Chem. Soc.* **2009,** 131, 15440-15456.
(23) Chaplin, A. B.; Weller, A. S. A rhodium (III) complex of the linear diborazine $H_3B\cdot NMe_2BH_2\cdot NMe_2H$: an intermediate in the dehydrocoupling of $H_3B\cdot NMe_2H$. *Acta Crystallogr. Sect. C.* **2011,** 67, 355-358.
(24) Bader, R. F. Atoms in Molecules: a quantum theory, International series of monographs on chemistry, *Oxford University Press. Oxford.* **1990,** 22.
(25) Matta, C. F.; Boyd, R. J. An introduction to the quantum theory of atoms in molecules. *The Quantum Theory of Atoms in Molecules: From Solid State to DNA and Drug Design.* **2007.** Edited by C.F. Matta and R.J. Boyd, WILEY-VCH, Weinham.
(26) Becke A.D; Edgecombe K. E. A simple measure of electron localization in atomic and molecular systems. J. Chem. Phys. **1990,** 92, 5397-5403.
(27) Bretschneider, E. S.; Allen, C. W. Reactions of the cis-1,2-dicyanoethylenedithiolate ion with disubtituted group IV organometallic compounds. *Inorg. Chem.* **1973,** 12, 623-627.
(28) Liu, F. C.; Plečnik, C. E.; Liu, S.; Liu, J.; Meyers, E. A.; Shore, S. G. Cyclic organohydroborate complexes of metallocenes: Part VI. Syntheses and structures of $Cp_2M\{(\mu\text{-}H)_2BR_2\}$(M=Ti,Nb; $R_2=C_4H_8,C_5H_{10},C_8H_{14}$). *J. Organomet. Chem.* **2001,** 627, 109-120.
(29) Chase, P. A.; Piers, W. E.; Parvez, M. Reactions of Bis(pentafluorophenyl)borane with Titanocene Dialkyls: Synthesis and Structure of $Cp_2Ti[\eta^2\text{-}H_2B(C_6F_5)_2]$. *Organometallics.* **2000,** 19, 2040-2042.
(30) Bader, R. F. Atoms in Molecules: a quantum theory, International series of monographs on chemistry, *Oxford University Press. Oxford.* **1990,** 22.
(31) Matta, C. F.; Boyd, R. J. An introduction to the quantum theory of atoms in molecules. *The Quantum Theory of Atoms in Molecules: From Solid State to DNA and Drug Design.* **2007.**
(32) Becke A.D; Edgecombe K. E. A simple measure of electron localization in atomic and molecular systems. J. Chem. Phys. **1990,** 92, 5397-5403.
(33) Lein M. Characterization of agostic interactions in theory and computation. *Coord. Chem. Rev.* **2009,** 253, 625-634.
(34) Popelier, P. L. A.; Logothetis, G. Characterization of an agostic bond on the basis of the electron density. J. Organomet. Chem. **1998,** 555, 101-111.
(35) Alvarez, M. A.; García-Vivó, D.; García, M. E.; Martínez, M. E.; Ramos, A.; Ruiz, M. A. Reactivity of the α-Agostic Methyl Bridge in the Unsaturated Complex $[Mo_2(\eta^5\text{-}C_5H_5)_2(\mu\text{-}\eta^1\text{:}\eta^2\text{-}CH_3)(\mu\text{-}PCy_2)(CO)_2]$: Migratory Behavior and Methylidyne Derivatives. *Organometallics.* **2008,** 27, 1973-1975.
(36) Noury, S.; Colonna, F.; Savin, A.; Silvi, B. Analysis of the delocalization in the topological theory of chemical bond. *J. Mol. Struct.* **1998,** 450, 59-68.
(37) Gaussian 09, Revision E.01, Frisch M. J.; Trucks G.W.; Schlegel H. B.; Scuseria G. E.; Robb M.A.; Cheeseman J. R.; Scalmani G.; Barone V.; Mennucci B.; Petersson G. A.; Nakatsuji H.; Caricato M.; Li X.; Hratchian H. P.; Izmaylov A. F.; Bloino J.; Zheng G.; Sonnenberg J. L.; Hada M.; Ehara M.; Toyota K.; Fukuda R.; Hasegawa J.; Ishida M.; Nakajima T.; Honda Y.; Kitao O.; Nakai H.; Vreven T.; Montgomery J. A.; Peralta J. E.; Ogliaro F.; Bearpark M.; Heyd J. J.; Brothers E.; Kudin K. N.; Staroverov V. N.; Kobayashi R.; Normand J.; Raghavachari K.; Rendell A.; Burant J.C.; Iyengar S. S.; Tomasi J.; Cossi M.; Rega N.; Millam J. M.; Klene M.; Knox J. E.; Cross J. B.; Bakken V.; Adamo C.; Jaramillo J.; Gomperts R.; Stratmann R. E.; Yazyev O.; Austin A. J.; Cammi R.; Pomelli C.; Ochterski J. W.; Martin R. L.; Morokuma K.; Zakrzewski V. G.; Voth G. A.; Salvador

P.; Dannenberg J. J.; Dapprich S.; Daniels A. D.; Farkas Ö.; Foresman J.B.; Ortiz J.V.; Cioslowski J.; Fox D. J. **2009,** Gaussian, Inc, Wallingford CT

(38) Zhu, J., Zins, E. L., & Alikhani, M. E. Characterization of BH agostic compounds involved in the dehydrogenation of amine-boranes by group 4 metallocenes. *Journal of molecular modeling*, **2016**, 22, 294.

(39) Becke, A. D. Density-functional exchange-energy approximation with correct asymptotic behavior. *Phys. Rev. A*, **1988,** 38, 3098.

(40) Lee, C.; Yang, W.; Parr, R. G. Development of the Colle-Salvetti correlation-energy formula into a functional of the electron density. *Phys. Rev. B*, **1988,** 37, 785.

(41) Jorge, F. E.; Canal Neto, A.; Camiletti, G. G.; Machado, S. F. Contracted Gaussian basis sets for Douglas–Kroll–Hess calculations: estimating scalar relativistic effects of some atomic and molecular properties. *J. Chem. Phys.* **2009,** 130, 064108.

(42) Neto, A. C.; Jorge, F. E. All-electron double zeta basis sets for the most fifth-row atoms: Application in DFT spectroscopic constant calculations. *Chem. Phys. Lett.* **2013,** 582, 158-162.

(43) Barros, C. L.; de Oliveira, P. J. P.; Jorge, F. E. ; Canal Neto, A.; Campos, M. Gaussian basis set of double zeta quality for atoms Rb through Xe: Application in non-relativistic and relativistic calculations of atomic and molecular properties. *Mol. Phys.* **2010,** 108, 1965-1972.

(44) Grimme, S.; Steinmetz, M. Effects of London dispersion correction in density. *Phys. Chem. Chem. Phys.* **2013,** 15, 16031-16042

(45) Lu, T.; Chen, F. Multiwfn: a multifunctional wavefunction analyzer. *J. Comput. Chem.* **2012,** 33, 580-592.